Biased agonism of carvedilol in the β_1-adrenergic receptor is governed by conformational exclusion

Layara Akemi Abiko,[1,4]* Ivana Petrovic,[1,4] Meltem Tatli,[2,3], Samit Desai[1], Henning Stahlberg,[2,3] Anne Spang[1], and Stephan Grzesiek[1]*

[1]Biozentrum, University of Basel, CH-4056 Basel, Switzerland

[2]Laboratory of Biological Electron Microscopy, Institute of Physics, School of Basic Sciences, Ecole Polytechnique Fédérale de Lausanne, CH-1015 Lausanne, Switzerland

[3]Laboratory of Biological Electron Microscopy, Department of Fundamental Microbiology, Faculty of Biology and Medicine, University of Lausanne, CH-1015 Lausanne, Switzerland

[4]These authors contributed equally

*Address correspondence to:
Layara Abiko
Structural Biology and Biophysics, Biozentrum
University of Basel, CH-4056 Basel, Switzerland
Phone: ++41 61 267 2100
FAX: ++41 61 267 2109
Email: layaraakemi.abiko@unibas.ch

Stephan Grzesiek
Structural Biology and Biophysics, Biozentrum
University of Basel, CH-4056 Basel, Switzerland
Phone: ++41 61 267 2100
FAX: ++41 61 267 2109
Email: Stephan.Grzesiek@unibas.ch

Keywords: G protein-coupled receptor; β_1-adrenergic receptor; carvedilol; arrestin2; biased agonism; structural biology.

ABSTRACT

G protein-coupled receptors (GPCRs) are the therapeutically most important family of receptors in the human genome. The selective activation of specific signaling pathways, termed biased signaling, is at the forefront of GPCR-targeted drug development[1]. These pathways are governed by dynamic equilibria among multiple GPCR conformations modulated by orthosteric ligands[2]. In this study, we elucidated the molecular mechanism underlying the biased signaling of carvedilol. This widely used beta-blocker is a heavily arrestin-biased agonist and at the same time, a G protein inverse agonist of β-adrenergic receptors (βARs)[3]. Our solution NMR, cryo-electron microscopy, and biochemical data show that the inactive conformation induced by carvedilol prevents G protein binding but is recognized by arrestin. Arrestin binding to the receptor is independent of the type and presence of orthosteric ligands, with the only requirement that arrestin is activated by a receptor phosphopeptide, which does not need to be covalently linked to the receptor. Thus, arrestin-biased signaling appears governed by conformational exclusion of the G protein in agreement with the promiscuous recognition of GPCRs by arrestin. The provided molecular details reveal the mechanism of selective transducer activation by GPCRs and provide new opportunities for developing safer therapeutics.

INTRODUCTION

G protein-coupled receptors (GPCRs) play a crucial role in regulating vital physiological processes, including vision, olfaction, cell migration, and immune responses[4]. They detect various orthosteric ligands, which modulate their conformational landscape and control the signaling to intracellular effectors. In addition to the canonical G protein-mediated signaling[5], GPCRs can also signal via arrestin proteins[6]. Arrestin binding to GPCRs requires phosphorylation of the receptor C-terminal tail or intracellular loops by GPCR kinases (GRKs)[7]. This interaction may then trigger numerous signaling pathways, which are independent of G-protein signaling, such as the activation of MAP-kinases[8].

Balanced orthosteric ligands prime the receptor to engage equally with G proteins and arrestins. Conversely, biased ligands preferentially stimulate the binding of one of these transducer proteins[9,10]. The functional selectivity of biased ligands is a promising avenue for developing novel drugs with tailored pharmacology, which may reduce side effects from the activation of unintended pathways[1,11,12]. One example of this approach is the recent demonstration that the selective blockage of arrestin-mediated GPR3 signaling ameliorates Alzheimer's disease pathology without affecting basal anxiety levels or cognitive function[13].

Although the benefits of biased drugs are well known, the structural determinants of fine-tuned biased agonism remain unclear. Previous studies have attempted to understand the selectivity of arrestin binding from the comparison of matched pairs of GPCR–G protein and GPCR–arrestin structures determined by crystallography or cryo-electron microscopy (cryo-EM)[14–19]. However, the structural differences between these arrestin and G protein complexes are minor. An alternative approach is the analysis of conformational differences in binary receptor complexes with ligands of differing pharmacology and selectivity[20–24]. Some of these studies implied specific receptor conformations associated with arrestin bias[20,22], while others proposed that arrestin may interact with multiple receptor conformations[21]. Therefore, no general mechanism for transducer protein selection has been determined.

Carvedilol is a heavily biased arrestin agonist targeting β_1- and β_2-adrenergic receptors[3]. Unlike other weakly biased ligands, carvedilol acts as an inverse agonist for G protein signaling while acting as an agonist for arrestin signaling[3]. This makes carvedilol an ideal model for studying biased agonism in GPCRs. To unravel how GPCRs may selectively activate certain cellular pathways, we have characterized the requirements for arrestin engagement to the β_1-adrenergic receptor (β_1AR) and compared the conformational changes of the carvedilol-bound receptor in the absence of transducer proteins and in the presence of arrestin2 or G protein mimicking proteins in solution. The observed molecular details explain the preferential binding of arrestin2 over G protein to the carvedilol•β_1AR complex.

RESULTS

β_1AR forms a stable complex with arrestin2 in the presence of unligated V2Rpp, independent of orthosteric ligands

The phosphosite density and distribution within the receptor C-terminal tail and intracellular loop 3 regulate the affinity of GPCRs towards arrestin proteins[25,26]. As a consequence of its high phosphosite density, the C-terminal tail of the vasopressin receptor 2 (V2R) forms well-characterized and stable complexes with arrestins[27–29]. For this reason, most structural studies of GPCR-arrestin complexes have been carried out on C-terminally truncated GPCRs fused via a sortase reaction[30] with a synthetic phosphorylated V2R C-terminal peptide (V2Rpp)[14,16] or coexpressed as a C-terminal V2Rpp chimera[19,31]. Due to the intrinsic dynamics of arrestin, many of these GPCR-arrestin complex structures have additionally been stabilized by Fab30[14,16,19] or ScFv30[28,31] antibody fragments. V2Rpp exhibits a relatively high affinity towards arrestin2 ($K_D \approx 20\ \mu M$)[25]. The interaction between V2Rpp and arrestin leads to arrestin activation via the release of the arrestin β20 strand and the subsequent reorientation of its N- and C-domains and core loops[29].

We analyzed the interactions of the isolated V2Rpp peptide, arrestin2 and β_1AR in presence and absence of orthosteric ligands by size exclusion chromatography (SEC, Fig. 1a). Surprisingly, the V2Rpp-activated arrestin2 forms a stable complex at low micromolar affinity with carvedilol-bound β_1AR

even in the absence of chemical ligation between the V2Rpp peptide and the receptor. The SEC data indicate that β_1AR•arrestin2 complex formation requires the presence of V2Rpp (Fig. 1a) and depends on the concentration of arrestin2 (Fig. 1b). Importantly, the complex formation does not depend on the presence of orthosteric ligands or their pharmacological properties, since apo β_1AR, isoprenaline (agonist)-bound β_1AR or cyanopindolol (antagonist)-bound β_1AR form the complex with arrestin2•V2Rpp in the same way as carvedilol-bound β_1AR (Fig. 1c).

A cryo-EM analysis of the carvedilol•β_1AR•arrestin2•V2Rpp preparation without addition of stabilizing antibodies revealed a well-formed complex with density visible in 2D classes both for the receptor and arrestin2 (Fig. 1d and S1). The flexibility of arrestin2 relative to the receptor did not allow a refinement of the complex to high resolution. However, the data were sufficient to yield a low-resolution 3D model of the complex (Fig. 1e and S1).

As phosphorylation appears to be the main driving force of receptor-arrestin interaction, we tested whether carvedilol has the ability to stimulate β_1AR phosphorylation in HEK293A cells expressing β_1AR fused to V2Rpp (Figs. 1f and S2). Similar to previous results for a β_2AR-V2Rpp fusion[3], carvedilol increased phosphorylation twofold relative to the basal signal in the absence of ligands. As expected, the β_1AR-V2Rpp phosphorylation stimulated by carvedilol corresponds to 20% of the phosphorylation induced by the full agonist isoprenaline.

Activation by V2Rpp primes arrestin2 for complex formation with β_1AR

Our findings suggest that the driving force for the β_1AR•arrestin2•V2Rpp complex formation is the phosphorylation-induced conformational change within arrestin2 resulting in enhanced interactions with the receptor core and not the attraction of arrestin2 towards the phosphorylated C-terminus of the receptor. We further tested this hypothesis by assessing the changes in the ^{1}H-^{13}C HMQC NMR spectrum of Ile-δ1-$^{13}CH_3$-labeled arrestin2 upon addition of V2Rpp (Fig. 2a). Ten-molar equivalents of the V2Rpp (corresponding to 95% of arrestin2 activation) caused significant chemical shift perturbations of isoleucine residues 31, 207, 214, 241, 314, 317, 318, and 386 (Figs. 2b and 2c). Whereas the change

in Ile386 is a direct consequence of the phosphopeptide binding and displacement of the β20 strand, the other affected residues are located at the interface between N- and C-domain of arrestin2. The latter chemical shift changes are consistent with the observation that phosphopeptide binding induces a change in the relative orientation between the two arrestin domains by ~20–25° as observed e.g. in V2Rpp•arrestin2[27] and CCR5 phosphopeptide•arrestin2[25] complexes and also in a V2Rpp•arrestin3[32] complex, indicative of the very similar activation mechanism of the two non-visual arrestin isoforms. Apparently, the phosphopeptide-induced release of strand β20 together with the change in relative domain orientation prime arrestin for interaction with the receptor core.

It is interesting to note that the Ile-δ1-$^{13}CH_3$ chemical shift perturbations in arrestin2 induced by the addition of V2Rpp are highly similar to those reported for arrestin2 in the presence of a β_2AR-V2Rpp chimera[33]. This indicates that the binding of arrestin2 to the receptor does not change the phosphopeptide-induced active arrestin2 conformation much further. Our solution state NMR findings are supported by almost identical structures of arrestin2 in phosphopeptide-bound[29] (PDB: 4JQI) and receptor-bound[14] (PDB:6TKO) forms.

Taken together, our data demonstrate that arrestin recruitment by β_1AR requires only the conformational change induced by phosphopeptide binding, but not a covalent attachment of the phosphopeptide to the receptor. The independence of the recruitment from the presence and pharmacological properties of orthosteric ligands (Fig. 1e) also shows that the activated arrestin is able to bind to multiple[14,34,35] – in particular G protein-active and -inactive – β_1AR conformations.

Arrestin recognizes both G protein binding-competent and -incompetent receptor states

To obtain further insights at atomic resolution into the conformation of β_1AR in the carvedilol•β_1AR•arrestin2•V2Rpp complex, we observed its ^{1}H-^{15}N tyrosine resonances by solution NMR. Tyrosines are excellent probes for the β_1AR functional state, as the rearrangement of the two conserved tyrosines Y^{5x58} and Y^{7x53} (superscripts indicate Ballesteros–Weinstein numbering[36]) is crucial for

receptor activation[34] (Fig. 3a). In the active state, the sidechains of both residues form a water-mediated bridge (YY-bridge closed). This YY-bridge is necessary for the transmembrane helices TM5 and TM6 to move outward to allow the accommodation of G proteins. In the inactive state, the YY-bridge is open and the opening of the intracellular helical bundle is reduced. The Y^{7x53} side chain is then rotated and interacts with the side chain amide of N^{7x49} within the NPxxY motif, whereas the Y^{5x58} side chain faces towards the intracellular opening of the transmembrane helix bundle.

The ^{1}H-^{15}N resonances of all nine β_1AR ^{15}N-tyrosine residues, including $Y227^{5x58}$ and $Y343^{7x53}$ (Fig. 3a), are observed in various ligand-bound states of the receptor (Figs. 3b-e, S3, and S4a). For the binary β_1AR complexes with the agonist isoprenaline or the inverse antagonist carvedilol, the ^{1}H-^{15}N resonances of $Y227^{5x58}$ and $Y343^{7x53}$ (Fig. 3b,e) are very similar and indicate an open YY-bridge. In contrast, both tyrosines undergo strong chemical shift changes in the active ternary complex with isoprenaline and the G protein mimicking nanobody Nb80, indicative of the formation of the closed YY-bridge that allows Nb80 binding.

Broader peaks are observed for the β_1AR•carvedilol•arrestin2•V2Rpp complex, in agreement with its increased molecular weight (~150 KDa including micelle) and dynamic nature (Fig. 3c,e). Due to the low sensitivity, also many natural abundance ^{15}N resonances of arrestin2 become observable. Nevertheless, the Y227 and Y343 resonances of this complex clearly have the same chemical shifts as the binary β_1AR•carvedilol complex with the open YY-bridge. Moreover, also the clearly detectable Y193, Y207, Y217, Y333 ^{1}H-^{15}N resonances are in positions which are identical to the binary β_1AR•carvedilol complex and distinctive for the inactive receptor. Hence the NMR data indicate that arrestin2 can recognize β_1AR in an inactive conformation with an open YY-bridge that is incompetent of G protein binding. The inability to bind to G protein is confirmed by the NMR spectra, which showed no changes and indication of complex formation for carvedilol-bound β_1AR when either the G protein mimicking Nb80 or miniGs (Figs. 3d, 3e, and S3) were added.

The open YY-bridge in the carvedilol•β_1AR•arrestin2•V2Rpp complex is very surprising since a previous structure of a formoterol•β_1AR•arrestin complex[12] had the YY-bridge in an identical closed conformation as in the respective G protein complex[12]. However, although formoterol is a weakly arrestin-biased agonist, in contrast to carvedilol, it also stimulates cAMP production at levels similar to those produced by G protein agonists[37]. Hence G protein activation is induced by this ligand and consistent with the closed YY-bridge.

Besides defining the state of the YY-bridge, the tyrosine ^{1}H-^{15}N resonances provide further insights into the response of the receptor to various ligands. Particularly strong changes between the G protein inactive carvedilol•β_1AR and the active isoprenaline•β_1AR•Nb80 complexes are observed for Y140^{3x51}, Y217^{5x48}, Y231^{5x62}, and Y333^{7x42} (Fig. 3b). As observed previously for several ^{15}N-valine residues[34,35,38], also Y333^{7x42} in the binary isoprenaline•β_1AR complex undergoes slow (≫millisecond) exchange between the preactive and the active conformation. A single conformation for all tyrosine residues is observed for the carvedilol•β_1AR complex. Interestingly, the complex with the antagonist cyanopindolol undergoes slow exchange between the inactive and preactive conformation for Y333^{7x42} located in TM7 (Fig. S4a), which has been implicated in arrestin signaling[21,24,39]. Presumably, the reduced conformational heterogeneity of TM7 in the carvedilol complex is caused by an additional hydrogen bond between carvedilol and the Y333^{7x42} sidechain (Fig. S4b). This hydrogen bond is absent in the complex with cyanopindolol (Fig. S4c).

Y227 and Y343 are not required for arrestin2 binding

The conserved Y227^{5x58} and Y343^{7x53} tyrosines are essential for G-protein binding[34]. To investigate their significance for the arrestin interaction, we generated a β_1AR mutant (β_1AR^{Y227A,Y343L}) lacking these residues. Remarkably, the β_1AR^{Y227A,Y343} mutant also forms a stable complex with the V2Rpp-activated arrestin2 as observed by SEC experiments (Fig. 4a). The sharper SEC profile and slightly reduced elution volume of this β_1AR^{Y227A,Y343L}•arrestin2•V2Rpp complex relative to the β_1AR•arrestin2•V2Rpp complex indicate an even higher

stability. As expected, no complex formation of $\beta_1AR^{Y227A,Y343L}$ was observed in the absence of V2Rpp (Fig. 4b).

The conformational state of $\beta_1AR^{Y227A,Y343L}$ in complex with arrestin2 was also characterized by NMR. For the binary complex of ^{15}N-valine labeled $\beta_1AR^{Y227A,Y343L}$ with carvedilol all expected 28 ^{1}H-^{15}N valine resonances are detected with high sensitivity in a ^{1}H-^{15}N TROSY spectrum (Fig. 4c). Upon addition of V2Rpp and arrestin2, all the valine resonances are dramatically broadened (Fig. 4c), as a result of the complex formation. The strongest ^{1}H-^{15}N resonances in this spectrum result from natural ^{15}N abundance of V2Rpp and arrestin2. However, all detected $\beta_1AR^{Y227A,Y343L}$ valine resonances are in positions corresponding to the inactive carvedilol binary-complex. This is expected since $\beta_1AR^{Y227A,Y343L}$ is unable to reach the active conformation[40].

DISCUSSION

To elucidate the mechanism of carvedilol-biased signaling towards arrestin, we have investigated the molecular details of arrestin2 recruitment to the β_1AR. Stable complexes of β_1AR and V2Rpp-activated arrestin2 could be generated in the absence of chemical ligation of V2Rpp with the receptor and without stabilizing antibody fragments. The independence of the arrestin interaction from the phosphopeptide-receptor ligation implies that the receptor•arrestin complex formation is not driven by the attraction of arrestin to the phosphorylated C-terminal tail or intracellular loops, but rather by the arrestin conformational rearrangement induced by the phosphopeptide, which enables the subsequent interaction of the activated arrestin with the receptor core.

The complex formation is also independent of receptor stimulation by an orthosteric ligand and its G protein agonistic or antagonistic properties. This agrees with previous findings that an arrestin core mutation (R169E in arrestin2), which activates arrestin in the absence of phosphopeptides, promotes interaction with GPCRs[41] and that such a constitutively active arrestin induces agonist-independent internalization of the 5-HT_{2A} serotonin receptor[42].

To shed light onto how β_1AR specifically interacts with either G protein or arrestin2, we investigated the conformational state of the YY-bridge. The primary

hallmark of the G protein active state of GPCRs is the pronounced outward movement of the intracellular end of TM6. This conformation is stabilized by a water-mediated bridge between Y^{5x58} and Y^{7x53} (YY-bridge closed) for adrenergic receptors (β_1AR – PDB 6H7J[43] and 6IBL[14], β_2AR – PDB 7BZ2). The existing structure of β_1AR complex with arrestin shows the YY-bridge is in the same active closed conformation as in the G protein complex (PDB 6TKO[14]). However, these structures have been solved with a G protein-activating orthosteric ligand. Here, we demonstrated by ^{1}H-^{15}N tyrosine NMR that the YY-bridge is open in the carvedilol•β_1AR•arrestin2•V2Rpp complex (Fig. 3e). Mutations of the $Y227^{5x58}$ and $Y343^{7x53}$ residues, which are essential for G protein binding, did not impair V2Rpp-activated arrestin2 recruitment by carvedilol-bound β_1AR (Fig. 4). To rationalize these findings, we propose that not the positive bias of the carvedilol-bound β_1AR for arrestin binding, but rather the negative bias against G protein binding via conformational exclusion explains arrestin-biased signaling (Fig. 5).

The presence of a phosphorylated peptide, albeit not necessarily covalently attached, is a prerequisite for arrestin binding to the receptor. We observed that carvedilol is able to induce the phosphorylation of a β_1AR-V2Rpp fusion in HEK293A cells. This agrees with cellular assays on a β_2AR-V2Rpp fusion[3] or wild-type β_1AR[44], in which phosphorylation by GRK and subsequent arrestin recruitment was induced by agonists and carvedilol, but not by other G protein inverse agonists (see Table S2). Corroborating our observations for $\beta_1AR^{Y227A,Y343L}$, also a G protein-inactive β_2AR-V2Rpp mutant ($T68^{2x39}F$, $Y132^{3x51}G$, $Y219^{5x58}A$) induced the same arrestin signaling and phosphorylation profile as the wild-type construct[3].

Conformational exclusion of G protein binding as the principle of arrestin bias is also in agreement with the high promiscuity of arrestin towards various GPCRs in different functional states. Indeed, in contrast to G protein, arrestin engaged with multiple receptor conformations in molecular dynamics simulations of the AT_1R receptor[39]. One of these conformations exclusively bound to arrestin with the Y^{7x53} side chain pointing towards the receptor intracellular opening and was thus incompetent for G protein binding. Moreover, recent arrestin2 complex

structures of the neurotensin receptor 1 (NTSR1)[45] and the class B glucagon receptor (GCGR)[31] also have the receptors in G protein-inactive conformations: whereas the NTSR1 Y^{7x53} side chain is in a conformation incompatible with G protein binding[45], GCGR is in a completely inactive conformation with arrestin2 making only contacts with TM8 and the C-terminal tail, but not with the receptor core[31]. This ability of arrestin to recognize multiple receptor conformations may also explain why only two non-visual arrestin isoforms are capable of regulating the hundreds of non-visual GPCRs[6].

Low-resolution experimental data by double electron-electron resonance spectroscopy[21] and ^{19}F-NMR[24] as well as molecular dynamics simulations[39] have shown a pivotal role of TM7 in arrestin bias. Our ^{1}H-^{15}N tyrosine NMR observations provide further details on the conformational state of TM7 in response to orthosteric ligands. Besides defining the state of the YY-bridge via the $Y343^{7x53}$ detection, the $Y333^{7x42}$ resonances indicate plasticity between inactive and active conformations for the $Y333^{7x42}$ backbone in the isoprenaline, isoprenaline•Nb80, and cyanopindolol complexes. In contrast, the $Y333^{7x42}$ backbone is tightly locked in the inactive conformation in the carvedilol complex, which can be rationalized by an additional hydrogen bond between carvedilol and the $Y333^{7x42}$ sidechain. Thus carvedilol specifically stabilizes the inactive conformation in this TM7 region thereby contributing to its arrestin-biased agonism.

Our high-resolution data on the interactions between β_1AR and arrestin in solution reveal conformational exclusion combined with phosphorylation as the mechanism governing arrestin-biased signaling. Arrestin recruitment is not controlled by the receptor conformation, but rather by its phosphorylation, which activates arrestin independent of direct receptor attachment of the phosphoresidues. By tightly controlling the conformational state of β_1AR, the biased ligand carvedilol prevents G protein binding while still inducing receptor phosphorylation, which allows the highly promiscuous, activated arrestin to engage effectively (Fig. 5). These detailed molecular insights on the mechanism

of biased signaling may facilitate the development of therapies targeted towards specific GPCR signaling pathways.

METHODS

Protein expression and purification

The expression of unlabelled, ^{15}N-valine-labeled, or ^{15}N-tyrosine-labeled turkey β_1AR, as well as of its G protein binding-incompetent variant ($\beta_1AR^{Y227A,Y343L}$) in baculovirus-infected Sf9 cells, purification, binding of ligands, and assignments were carried out as described previously[34,40,46].

Unlabelled arrestin2 (residues 1-393) expression and purification were performed as described before[25]. For the preparation of Ile-δ1-$^{13}CH_3$-labeled arrestin2, the *E. coli* (BL21) cells were grown in D_2O M9 minimal medium supplemented with 80 mg per liter of 2-ketobutyric acid-4-^{13}C,3,3-d_2 sodium salt hydrate following previously reported procedures[47].

The plasmids for Nb80 and MiniGs were generous gifts by Dr. Jan Steyaert and Dr. Chris Tate, respectively. Nb80 and MiniG_S were produced according to described procedures[48,49].

Peptide synthesis

The phosphorylated V2R peptide (V2Rpp, ARGRpTPPpSLGPQDEpSCpTpTApSpSpSLAKDTSS) corresponding to the last 29 residues of the Vasopressin receptor 2 was obtained from the Tufts University Core Facility for peptide synthesis.

Size exclusion chromatography

SEC binding assays were performed on an UltiMate 3000 HPLC system using a self-packed 4.2-mL S200 10/300 SEC column (length 25 mm, diameter 4.6 mm) pre-equilibrated with SEC buffer (20 mM Tris-HCl, 100 mM NaCl, ~40 mM decylmaltoside (DM), 0.02% NaN_3, pH 7.5). Samples containing 20 μM β_1AR (1x), 40 μM arrestin2 (2x), 100 μM V2Rpp (5x) and 1 mM (carvedilol, cyanopindolol) or 2 mM (isoprenaline) ligand were prepared as 270 μL volumes in SEC buffer. The SEC buffer was supplemented with 10 μM carvedilol, 10 μM cyanopindolol or 1 mM isoprenaline, respectively. Control β_1AR and arrestin2 samples were prepared at the same concentrations as in the sample mixtures.

Cryo-EM sample preparation and grid freezing

The carvedilol•β_1AR•arrestin2•V2Rpp complex for cryo-EM analysis was prepared similarly to the samples for the SEC-binding assay. Samples were prepared as 270 µL volumes and contained 50 µM receptor, 100 µM arrestin2, 250 µM V2Rpp and 1 mM carvedilol. The samples were incubated for 30 min on ice before injecting onto the 4.2 mL SEC column preeqilibrated with cryo-EM buffer (20 mM HEPES, 100 mM NaCl, 0.01 % LMNG, pH 7.5, 10 µM carvedilol). The SEC fractions were checked using SDS-PAGE, correct fractions pooled and concentrated to 1.4 mg/ml.

Cryo-EM data collection and structure determination

3-µl aliquots of the sample were deposited onto glow-discharged Quantifoil™ R1.2/1.3 (Cu) or R2/1 (Gold) grids and rapidly frozen in liquid ethane using a Leica EM GP2 plunger adjusted to +4°C and 80% humidity, with a blotting time of 3-5 seconds. Data acquisition as Electron Event Recordings (EER) was performed on a TFS Titan Krios G4 microscope, equipped with a cold-FEG electron source and Falcon4i camera (DCI-Lausanne), detailed in Table S1.

Recorded EER files were processed in RELION 4.0[50,51]. Motion correction was performed usin RELION's implementation of Motioncor2, with 32 EER fractions per movie frame. CTF estimation was conducted using CTFFIND 4.1.14[52], with selection criteria based on a maximum CTF resolution of better than 6 Å and defocus between 0.5 to 2.5 µm. Particle picking utilized template matching or blob picking methods, yielding a large particle dataset (**Table S1**). The particle stacks were imported to cryoSPARC[53] and rounds of 2D classification were carried. Good 2D classes were used for ab initio model generation, and refined using non-uniform refinement in cryoSPARC. The volumes were visualized in ChimeraX[54].

NMR experiments

NMR samples were prepared with typical receptor concentrations of 100−200 µM in 20 mM Tris-HCl, 100 mM NaCl, ~40 mM decylmaltoside (DM), 0.02% NaN_3, 5% D_2O, pH 7.5. Binary complexes with the various orthosteric ligands were formed by adding 2 mM ligand. For isoprenaline, 20 mM sodium

ascorbate was added to prevent oxidation. Ternary complexes were formed by adding a 1.2-molar equivalent of Nb80, a 1.5-molar equivalent of $MiniG_S$, or a 1.5-molar equivalent of arrestin2 together with a 5-molar equivalent of V2Rpp, respectively.

^{1}H-^{15}N TROSY NMR experiments were recorded on Bruker AVANCE 900 MHz or AVANCE 600 MHz spectrometers equipped with TCI cryoprobes at 304 K using sample volumes of ~250 µL in Shigemi microtubes. ^{1}H-^{15}N TROSY experiments were recorded as 80 (^{15}N) × 1024 (^{1}H) complex points with acquisition times of 16 ms (^{15}N) and 42 ms (^{1}H). For optimal sensitivity, the ^{1}H-^{15}N transfer time was reduced to 3.0 ms and a 1 s interscan delay was used. Typical total experimental times were 48 h.

A titration of 50 µM Ile-δ1-$^{13}CH_3$, ^{2}H-labeled arrestin2 with V2Rpp up to a concentration of 500 µM was monitored by ^{1}H-^{13}C HMQC spectra. The assignments of the methyl groups were transferred from BMRB ID:51131[33]. Chemical shift perturbations (CSP) were calculated from Equation 1, where $\Delta\delta_H$ is the methyl proton chemical shift difference, and $\Delta\delta_{13C}$ is the ^{13}C-methyl chemical shift difference between the apo and bound states.

$$\mathrm{CSP} = \sqrt{\Delta\delta_H{}^2 + \left(\frac{\Delta\delta_{13C}}{3.6}\right)^2} \quad (1)$$

CSPs larger than the average CSP calculated from all resonances were considered significant.

All NMR spectra were processed with NMRPipe[55] and evaluated with CcpNmr Analysis[56] or NMRFAM-SPARKY[57]. 1D-NMR traces were generated using the nmrglue[58] module in the PyCharm environment (JetBrains, PyCharm 2020.1.2).

Structural analysis

Molecular visualization was carried out with UCSF ChimeraX[59].

Cellular assays

HEK293A cells were grown in high-glucose Dulbecco's modified Eagle's medium (Sigma-Aldrich) with 10% fetal bovine serum (FBS, Biowest), 2 mM L-

glutamine, 100 U ml^{-1} penicillin G and 100 ng ml^{-1} streptomycin, 1 mM sodium pyruvate at 37 °C and 5% CO_2.

To asses the level of phosphorylation of the receptor, cells were plated into six-well plates to reach 70% confluency. Cells were transfected with 0.3 µg of each arrestin2-YFP and β_1AR-V2Rpp plasmid DNA (GenScript) complexed with Helix-IN transfection reagent (OZ Biosciences). Transfection was carried out according to the manufacturer's recommendation. Post 24 hours of transfection, cells were treated with 100 µM of isoprenaline (positive control) and 10 µM of carvedilol for 30 minutes. Cells were lysed using RIPA buffer (50mM Tris pH 8, 150 mM NaCl, 5 mM EDTA, 0.5% sodium deoxycholate, 0.1 % SDS, 1 % Triton X-100) supplemented with 1x Halt's protease and phosphatase inhibitor cocktail.

Phosphorylation and total amount of flag-tagged β_1AR-V2Rpp were quantified by western blotting using chemiluminescence. For this, 20 µL of the respective fractions were diluted with 5 µL SDS–PAGE buffer (125 mM Tris–HCl pH 6.8, 4% (w/v) SDS, 20% (v/v) glycerol and 0.01% (w/v) bromophenol blue) and loaded onto Mini-PROTEAN TGX™ 4–20% precast gels (Bio-Rad). As a reference, 3 µL of Precision Plus Protein™ dual color standard weight ladder (#1610374, Bio-Rad) were also loaded onto the gel, and the proteins separated for 30 min at 200 V. Proteins were transferred to 0.2 µm nitrocellulose membranes using the Trans-Blot Turbo™ transfer system (Bio-Rad). Western-blot membranes were blocked with 1% BSA in Tris-Buffered Saline-Tween (TBST) for 1 h and then incubated with monoclonal HRP anti-flag tag antibody (1:5000 dilution, Thermo Fisher) or with primary (rabbit polyclonal) phospho-V2R [pT359/pT360] antibody (1:2000 dilution, 7TM antibodies) followed by HRP-coupled anti-rabbit secondary antibody (1:5000 dilution, Thermo Fisher) for 1 hour each. Blots were then washed three times for 5 min with TBST and developed using the Lumi-Light Western Blotting Substrate (Hoffmann-La Roche). The chemiluminescence signal was detected using a Fusion FX6 reader (Vilber) at 600 dpi resolution. Individually selected bands of the obtained images from the western blot membranes were quantified by ImageJ[60] after background subtraction using the

rolling ball radius method (90 pixels). Phosphorylation levels were normalized using the respective total amount of expressed flag-tagged β_1AR-V2Rpp.

Statistics

A statistical analysis of cellular receptor phosphorylation was performed using GraphPad Prism 10.1.1 (GraphPad Software, Inc., San Diego, CA, USA). The normality of the individual ligand-induced phosphorylation results was tested using the Shapiro-Wilk normality test and the data were cross-compared using an ordinary one-way ANOVA test.

DATA AVAILABILITY

The Cryo-EM density map for β_1AR in complex with carvedilol, arrestin2, and V2Rpp was deposited to the Electron Microscopy Data Bank (EMDB) with accession code EMDB-50623 and the raw cryo-EM images were deposited to the Electron Microscopy Public Image Archive (EMPIAR) with accession code EMPIAR-12139.

ACKNOWLEDGMENTS

This work was supported by the Swiss National Science Foundation (grants CRSK-3_195592 to L.A.A., and 31-201270 and IZLIZ3-200298 to S.G, 310030-188548 to HS, and 310030-197779 to A.S), and by a Fellowship for Excellence by the Biozentrum Basel International PhD Program to I.P. We gratefully acknowledge Drs. Timothy Sharpe and Tobias Mühlethaler (Biozentrum Biophysics Facility) for expert help with the biophysical characterization of β_1AR, Drs. Mohamed Chami, Carlos Fernandez Rodriguez, and Carola Alampi (Biozentrum BioEM lab) for cryo-EM initial screenings, the Dubochet Center for Imaging Lausanne (a joint initiative from EPFL, UNIGE, UNIL, UNIBE) with the assistance of Drs. A. Myasnikov, B. Beckert, S. Nazarov, I. Mohammed, and E. Uchikawa for cryo-EM data collection, as well as Dr. Timm Maier for helpful discussions.

AUTHOR CONTRIBUTIONS

L.A.A., I.P., and S.G. conceived the study. L.A.A. expressed and purified β_1AR and $\beta_1AR^{Y227A,Y343L}$, and recorded and analyzed NMR data on those proteins. I.P. expressed and purified arrestin2 and recorded and analyzed NMR data of

arrestin2 with V2Rpp. I.P. and L.A.A. designed SEC experiments and prepared complexes for EM. M.T. prepared EM grids and collected the EM data. M.T. and I.P. processed and analyzed the EM data. H.S. provided guidance on EM data collection, processing, and evaluation. S.D., L.A.A, and I.P. performed the cellular assays and analyzed the cellular data with guidance from A.S. L.A.A., I.P. and S.G. wrote the manuscript.

COMPETING INTERESTS STATEMENT

The authors declare no competing interests.

REFERENCES

1. Hauser, A. S., Attwood, M. M., Rask-Andersen, M., Schiöth, H. B. & Gloriam, D. E. Trends in GPCR drug discovery: new agents, targets and indications. *Nat Rev Drug Discov* **16**, 829–842 (2017).
2. Latorraca, N. R., Venkatakrishnan, A. J. & Dror, R. O. GPCR Dynamics: Structures in Motion. *Chem. Rev.* **117**, 139–155 (2017).
3. Wisler, J. W. *et al.* A unique mechanism of β-blocker action: Carvedilol stimulates β-arrestin signaling. *Proceedings of the National Academy of Sciences* **104**, 16657–16662 (2007).
4. Rosenbaum, D. M., Rasmussen, S. G. F. & Kobilka, B. K. The structure and function of G-protein-coupled receptors. *Nature* **459**, 356–363 (2009).
5. Weis, W. I. & Kobilka, B. K. The Molecular Basis of G Protein–Coupled Receptor Activation. *Annual Review of Biochemistry* **87**, 897–919 (2018).
6. Gurevich, V. V. & Gurevich, E. V. GPCR Signaling Regulation: The Role of GRKs and Arrestins. *Frontiers in Pharmacology* **10**, (2019).
7. Komolov, K. E. & Benovic, J. L. G protein-coupled receptor kinases: Past, present and future. *Cellular Signalling* **41**, 17–24 (2018).
8. McDonald, P. H. *et al.* β-Arrestin 2: A Receptor-Regulated MAPK Scaffold for the Activation of JNK3. *Science* (2000) doi:10.1126/science.290.5496.1574.
9. Wootten, D., Christopoulos, A., Marti-Solano, M., Babu, M. M. & Sexton, P. M. Mechanisms of signalling and biased agonism in G protein-coupled receptors. *Nat Rev Mol Cell Biol* **19**, 638–653 (2018).
10. Wingler, L. M. & Lefkowitz, R. J. Conformational Basis of G Protein-Coupled Receptor Signaling Versatility. *Trends in Cell Biology* **30**, 736–747 (2020).
11. Slosky, L. M., Caron, M. G. & Barak, L. S. Biased Allosteric Modulators: New Frontiers in GPCR Drug Discovery. *Trends in Pharmacological Sciences* **42**, 283–299 (2021).
12. Seyedabadi, M., Ghahremani, M. H. & Albert, P. R. Biased signaling of G protein coupled receptors (GPCRs): Molecular determinants of GPCR/transducer selectivity and therapeutic potential. *Pharmacol Ther* **200**, 148–178 (2019).

13. Huang, Y. *et al.* G protein–biased GPR3 signaling ameliorates amyloid pathology in a preclinical Alzheimer's disease mouse model. *Proceedings of the National Academy of Sciences* **119**, e2204828119 (2022).
14. Lee, Y. *et al.* Molecular basis of β-arrestin coupling to formoterol-bound β1-adrenoceptor. *Nature* **583**, 862–866 (2020).
15. Maeda, S., Qu, Q., Robertson, M. J., Skiniotis, G. & Kobilka, B. K. Structures of the M1 and M2 muscarinic acetylcholine receptor/G-protein complexes. *Science* **364**, 552–557 (2019).
16. Staus, D. P. *et al.* Structure of the M2 muscarinic receptor–β-arrestin complex in a lipid nanodisc. *Nature* **579**, 297–302 (2020).
17. Kato, H. E. *et al.* Conformational transitions of a neurotensin receptor 1–Gi1 complex. *Nature* **572**, 80–85 (2019).
18. Huang, W. *et al.* Structure of the neurotensin receptor 1 in complex with β-arrestin 1. *Nature* **579**, 303–308 (2020).
19. Liao, Y.-Y. *et al.* Snapshot of the cannabinoid receptor 1-arrestin complex unravels the biased signaling mechanism. *Cell* **186**, 5784-5797.e17 (2023).
20. Bumbak, F. *et al.* Stabilization of pre-existing neurotensin receptor conformational states by β-arrestin-1 and the biased allosteric modulator ML314. *Nat Commun* **14**, 3328 (2023).
21. Wingler, L. M. *et al.* Angiotensin Analogs with Divergent Bias Stabilize Distinct Receptor Conformations. *Cell* **176**, 468-478.e11 (2019).
22. Kleist, A. B. *et al.* Conformational selection guides β-arrestin recruitment at a biased G protein–coupled receptor. *Science* **377**, 222–228 (2022).
23. Wingler, L. M. *et al.* Angiotensin and biased analogs induce structurally distinct active conformations within a GPCR. *Science* **367**, 888–892 (2020).
24. Liu, J. J., Horst, R., Katritch, V., Stevens, R. C. & Wüthrich, K. Biased Signaling Pathways in β2-Adrenergic Receptor Characterized by 19F-NMR. *Science* **335**, 1106–1110 (2012).
25. Isaikina, P. *et al.* A key GPCR phosphorylation motif discovered in arrestin2•CCR5 phosphopeptide complexes. *Molecular Cell* **83**, 2108-2121.e7 (2023).
26. Oakley, R. H., Laporte, S. A., Holt, J. A., Barak, L. S. & Caron, M. G. Molecular determinants underlying the formation of stable intracellular G protein-coupled receptor-beta-arrestin complexes after receptor endocytosis*. *J Biol Chem* **276**, 19452–19460 (2001).
27. He, Q.-T. *et al.* Structural studies of phosphorylation-dependent interactions between the V2R receptor and arrestin-2. *Nat Commun* **12**, 2396 (2021).
28. Bous, J. *et al.* Structure of the vasopressin hormone-V2 receptor-β-arrestin1 ternary complex. *Sci Adv* **8**, eabo7761 (2022).
29. Shukla, A. K. *et al.* Structure of active β-arrestin-1 bound to a G-protein-coupled receptor phosphopeptide. *Nature* **497**, 137–141 (2013).
30. Staus, D. P. *et al.* Sortase ligation enables homogeneous GPCR phosphorylation to reveal diversity in β-arrestin coupling. *Proceedings of the National Academy of Sciences* **115**, 3834–3839 (2018).
31. Chen, K. *et al.* Tail engagement of arrestin at the glucagon receptor. *Nature* **620**, 904–910 (2023).

32. Maharana, J. *et al.* Structural snapshots uncover a key phosphorylation motif in GPCRs driving β-arrestin activation. *Molecular Cell* **83**, 2091-2107.e7 (2023).
33. Shiraishi, Y. *et al.* Biphasic activation of β-arrestin 1 upon interaction with a GPCR revealed by methyl-TROSY NMR. *Nat Commun* **12**, 7158 (2021).
34. Grahl, A., Abiko, L. A., Isogai, S., Sharpe, T. & Grzesiek, S. A high-resolution description of β1-adrenergic receptor functional dynamics and allosteric coupling from backbone NMR. *Nat Commun* **11**, 2216 (2020).
35. Abiko, L. A., Grahl, A. & Grzesiek, S. High Pressure Shifts the β1-Adrenergic Receptor to the Active Conformation in the Absence of G Protein. *J. Am. Chem. Soc.* **141**, 16663–16670 (2019).
36. Ballesteros, J. A. & Weinstein, H. [19] Integrated methods for the construction of three-dimensional models and computational probing of structure-function relations in G protein-coupled receptors. in *Methods in Neurosciences* (ed. Sealfon, S. C.) vol. 25 366–428 (Academic Press, 1995).
37. Rajagopal, S. *et al.* Quantifying Ligand Bias at Seven-Transmembrane Receptors. *Mol Pharmacol* **80**, 367–377 (2011).
38. Abiko, L. A. *et al.* Filling of a water-free void explains the allosteric regulation of the β1-adrenergic receptor by cholesterol. *Nat. Chem.* **14**, 1133–1141 (2022).
39. Suomivuori, C.-M. *et al.* Molecular mechanism of biased signaling in a prototypical G protein–coupled receptor. *Science* **367**, 881–887 (2020).
40. Isogai, S. *et al.* Backbone NMR reveals allosteric signal transduction networks in the β1-adrenergic receptor. *Nature* **530**, 237–241 (2016).
41. Gurevich, V. V. & Gurevich, E. V. The molecular acrobatics of arrestin activation. *Trends Pharmacol Sci* **25**, 105–111 (2004).
42. Gray, J. A., Bhatnagar, A., Gurevich, V. V. & Roth, B. L. The Interaction of a Constitutively Active Arrestin with the Arrestin-Insensitive 5-HT2A Receptor Induces Agonist-Independent Internalization. *Mol Pharmacol* **63**, 961–972 (2003).
43. Warne, T., Edwards, P. C., Doré, A. S., Leslie, A. G. W. & Tate, C. G. Molecular basis for high-affinity agonist binding in GPCRs. *Science* **364**, 775 (2019).
44. Kim, I.-M. *et al.* Beta-blockers alprenolol and carvedilol stimulate beta-arrestin-mediated EGFR transactivation. *Proc Natl Acad Sci U S A* **105**, 14555–14560 (2008).
45. Duan, J. *et al.* GPCR activation and GRK2 assembly by a biased intracellular agonist. *Nature* **620**, 676–681 (2023).
46. Wu, F.-J. *et al.* Nanobody GPS by PCS: An Efficient New NMR Analysis Method for G Protein Coupled Receptors and Other Large Proteins. *J. Am. Chem. Soc.* **144**, 21728–21740 (2022).
47. Tugarinov, V., Kanelis, V. & Kay, L. E. Isotope labeling strategies for the study of high-molecular-weight proteins by solution NMR spectroscopy. *Nat Protoc* **1**, 749–754 (2006).
48. Rasmussen, S. G. F. *et al.* Structure of a nanobody-stabilized active state of the β2 adrenoceptor. *Nature* **469**, 175–180 (2011).
49. Rößler, P. *et al.* GPCR Activation States Induced by Nanobodies and Mini-G Proteins Compared by NMR Spectroscopy. *Molecules* **25**, 5984 (2020).
50. Scheres, S. H. W. RELION: Implementation of a Bayesian approach to cryo-EM structure determination. *Journal of Structural Biology* **180**, 519–530 (2012).

51. Zivanov, J. *et al.* A Bayesian approach to single-particle electron cryo-tomography in RELION-4.0. *eLife* **11**, e83724 (2022).
52. Rohou, A. & Grigorieff, N. CTFFIND4: Fast and accurate defocus estimation from electron micrographs. *Journal of Structural Biology* **192**, 216–221 (2015).
53. Punjani, A., Rubinstein, J. L., Fleet, D. J. & Brubaker, M. A. cryoSPARC: algorithms for rapid unsupervised cryo-EM structure determination. *Nat Methods* **14**, 290–296 (2017).
54. Goddard, T. D. *et al.* UCSF ChimeraX: Meeting modern challenges in visualization and analysis. *Protein Science* **27**, 14–25 (2018).
55. Delaglio, F. *et al.* NMRPipe: A multidimensional spectral processing system based on UNIX pipes. *J Biomol NMR* **6**, 277–293 (1995).
56. Vranken, W. F. *et al.* The CCPN data model for NMR spectroscopy: Development of a software pipeline. *Proteins: Structure, Function, and Bioinformatics* **59**, 687–696 (2005).
57. Lee, W., Tonelli, M. & Markley, J. L. NMRFAM-SPARKY: enhanced software for biomolecular NMR spectroscopy. *Bioinformatics* **31**, 1325–1327 (2015).
58. Helmus, J. J. & Jaroniec, C. P. Nmrglue: an open source Python package for the analysis of multidimensional NMR data. *J Biomol NMR* **55**, 355–367 (2013).
59. Meng, E. C. *et al.* UCSF ChimeraX: Tools for structure building and analysis. *Protein Science* **32**, e4792 (2023).
60. Schindelin, J. *et al.* Fiji: an open-source platform for biological-image analysis. *Nature Methods* **9**, 676–682 (2012).

FIGURE LEGENDS

Fig. 1: β_1AR•arrestin•V2Rpp complex formation. a, SEC profiles of β_1AR+arrestin2+V2Rpp (red), β_1AR+arrestin (green), β_1AR (blue), and arrestin2 (yellow) solutions in the presence of carvedilol. **b,** SEC profiles of β_1AR+arrestin2+V2Rpp mixtures at different arrestin2:β_1AR molar ratios in the presence of carvedilol. **c,** SEC profiles of β_1AR+arrestin2+V2Rpp mixtures without orthosteric ligand (green) or in the presence of carvedilol (red), isoprenaline (blue), or cyanopindolol (purple). The concentrations of individual components in **a-c** are given in Methods. **d,** CryoEM 2D classes of carvedilol•β_1AR•arrestin2•V2Rpp complex. **e,** CryoEM 3D representation of carvedilol•β_1AR•arrestin2•V2Rpp complex. **f,** β_1AR-V2Rpp phosphorylation detected in HEK293A cells by pT359/pT360 phospho-antibodies in the absence and presence of isoprenaline and carvedilol ligands. Individual phosphorylation amounts relative to isoprenaline, as well as their mean and standard deviation of the mean are shown for N=3 biological replicates; ****: $P < 0.0001$; *: $P < 0.05$.

Fig. 2: Arrestin2 activation by V2Rpp. a, ^{1}H-^{13}C HMQC spectra of apo Ile-δ1-$^{13}CH_3$, ^{2}H-labeled arrestin2 (black) and upon addition of a 10-molar equivalent of the V2Rpp (red). Resonances marked with an asterisk could not be assigned in the bound state. **b,** Chemical shift perturbation (CSP) of arrestin2 isoleucine $^1H_3$-$^{13}C^{\delta 1}$ resonances upon addition of the V2Rpp phosphopeptide. The solid line depicts the average perturbation. **c,** AlphaFold2 model of arrestin2 showing the N- and C-domains (gray). Ile residues are indicated as spheres. The residues coloured in red undergo significant CSPs upon phosphopeptide addition.

Fig. 3: Detection of the β_1AR functional state by ^{1}H-^{15}N-tyrosine NMR. a, G protein-active and -inactive conformations of Y227^{5x58} and Y343^{7x53} in β_1AR. Left: full structure of active β_1AR (β_1AR•isoprenaline•Nb80 complex, PDB 6H7J) with all tyrosine residues indicated. Middle: active conformation of TM5 and TM7 with water-mediated (red sphere) bridge between Y227 and Y343 (YY-bridge closed). Right: inactive TM5/TM7 conformation (β_2AR•carvedilol complex, PDB 6PS3) with Y227 and Y343 separated (YY-bridge open). **b-d,** Superposition of ^{1}H-^{15}N TROSY spectra of ^{15}N-tyrosine-labeled β_1AR bound to different ligands and transducer proteins. Color codes are indicated in each panel. The tyrosine

resonances are marked with assignment information. Resonances connected by a dashed magenta line represent residues with two clearly distinguishable resonances for the inactive ('i') and active ('a') conformations. Resonances that are not assigned to any tyrosine are marked by an asterisk. **e,** Selected regions of the ^{1}H-^{15}N TROSY spectra showing the resonances of Y227 and Y343 for β_1AR in different complexes and functional states. The green dashed ellipses represent the absent active-conformation resonances. The structures above each spectrum depict the respective Y227 and Y343 conformations (PDB codes 6PS3, 6H7J, and 6TKO).

Fig. 4: The G protein binding-incompetent mutant β_1AR^{Y227A,Y343} binds arrestin2. a, SEC profiles of the carvedilol•β_1AR^{Y227A,Y343}•arrestin2•V2Rpp (orange) and carvedilol•β_1AR•arrestin2•V2Rpp (black) complexes. **b,** SEC profile of a 50:1:2 carvedilol:β_1AR^{Y227A,Y343L}:arrestin2 molar mixture in presence of a 5-molar V2Rpp equivalent (orange) or in its absence (blue). **c,** Left: superposition of ^{1}H-^{15}N TROSY spectra of ^{15}N-valine-labeled carvedilol•β_1AR complex in absence (blue) and presence of a 1.5-molar equivalent of arrestin2•V2Rpp complex (orange). Valine resonances are marked with assignment information. The severe broadening of the β_1AR valine resonances upon addition of arrestin2 and phosphopeptide indicates complex formation. Due to the line broadening, the sensitivity of the ^{15}N-valine detection is low in the quaternary complex, and natural abundance ^{15}N arrestin2 resonances (light orange) become dominant. The ^{15}N natural abundance TROSY spectrum of an arrestin2:V2Rpp 1:5 molar mixture (grey, single contour lines) is shown as a control. 1D traces through selected ^{1}H-^{15}N valine resonances are shown on the right and emphasize the line broadening due to complex formation.

Fig. 5: Structural basis of the carvedilol arrestin-biased agonism. Left: Balanced or weakly arrestin-biased agonists promote increased dynamics of the intracellular portion of the receptor, allowing the receptor to populate the G protein-active state of β_1AR with the conserved Y227 and Y343 (purple) in the closed conformation of the YY-bridge (green helices). This allows both G protein (green) and arrestin (red) to bind to the receptor. Right: strong arrestin-biased

agonists, such as carvedilol (red sticks), stabilize a G protein-inactive state, with Y227 and Y343 in the YY-bridge open conformation (red helices), which can only bind to arrestin but not to G proteins. The arrestin2 activated by V2Rpp (thick black line, phosphosites indicated as yellow spheres) is highly dynamic.

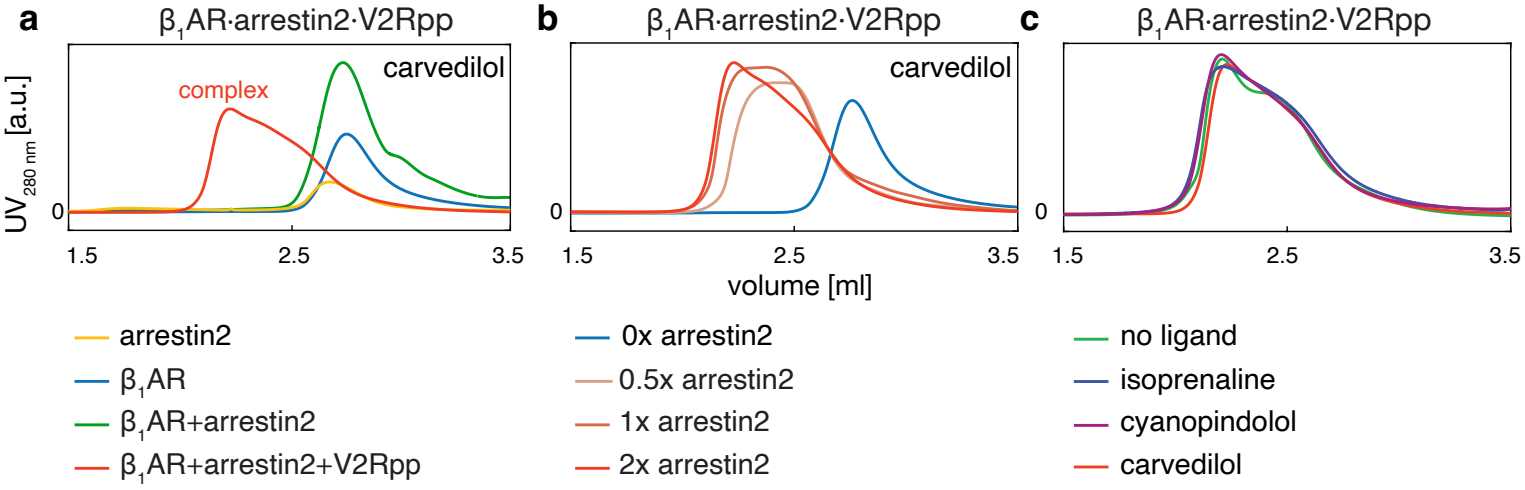
a
β1AR·arrestin2·V2Rpp
carvedilol
complex
UV280 nm [a.u.]
0
1.5
2.5
3.5
b
β1AR·arrestin2·V2Rpp
carvedilol
0
1.5
2.5
3.5
volume [ml]
c
β1AR·arrestin2·V2Rpp
0
1.5
2.5
3.5
arrestin2
β1AR
β1AR+arrestin2
β1AR+arrestin2+V2Rpp
0x arrestin2
0.5x arrestin2
1x arrestin2
2x arrestin2
no ligand
isoprenaline
cyanopindolol
carvedilol

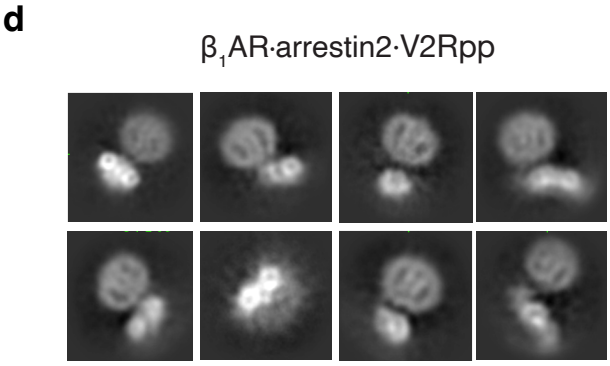
d
β1AR·arrestin2·V2Rpp

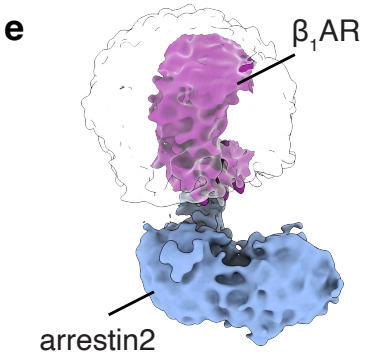
e
β1AR
arrestin2

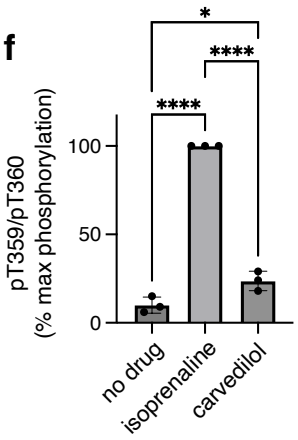
f
pT359/pT360
(% max phosphorylation)
100
50
0
****
****
*
no drug
isoprenaline
carvedilol

Figure 1

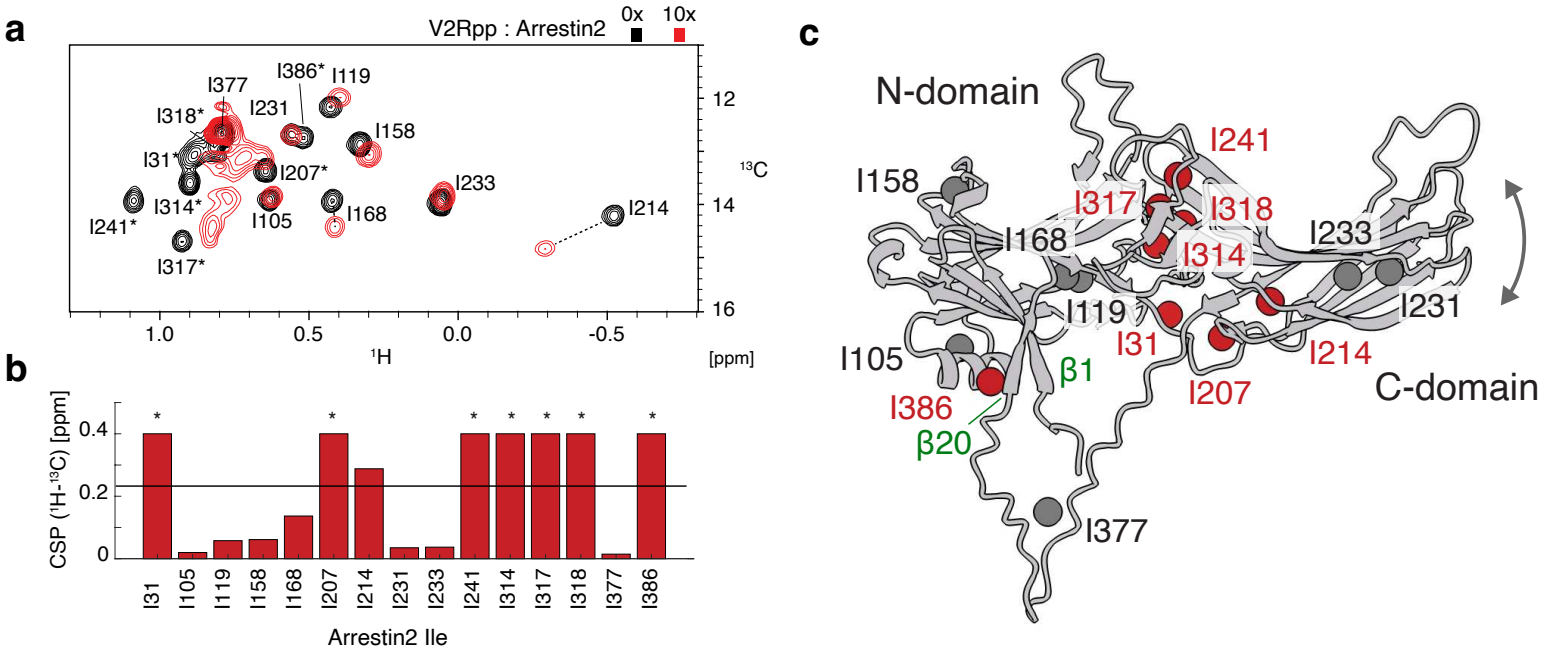
a
V2Rpp : Arrestin2
0x
10x
I377
I386*
I119
I318*
I231
I158
I31*
I207*
I233
I241*
I314*
I105
I168
I214
I317*
12
14
16
^{13}C
1.0
0.5
0.0
-0.5
^{1}H
[ppm]
b
CSP (^{1}H-^{13}C) [ppm]
0.4
0.2
0
I31
I105
I119
I158
I168
I207
I214
I231
I233
I241
I314
I317
I318
I377
I386
Arrestin2 Ile
c
N-domain
I241
I158
I317
I318
I168
I314
I233
I119
I231
I31
I105
I214
β1
I207
C-domain
I386
β20
I377

Figure 2

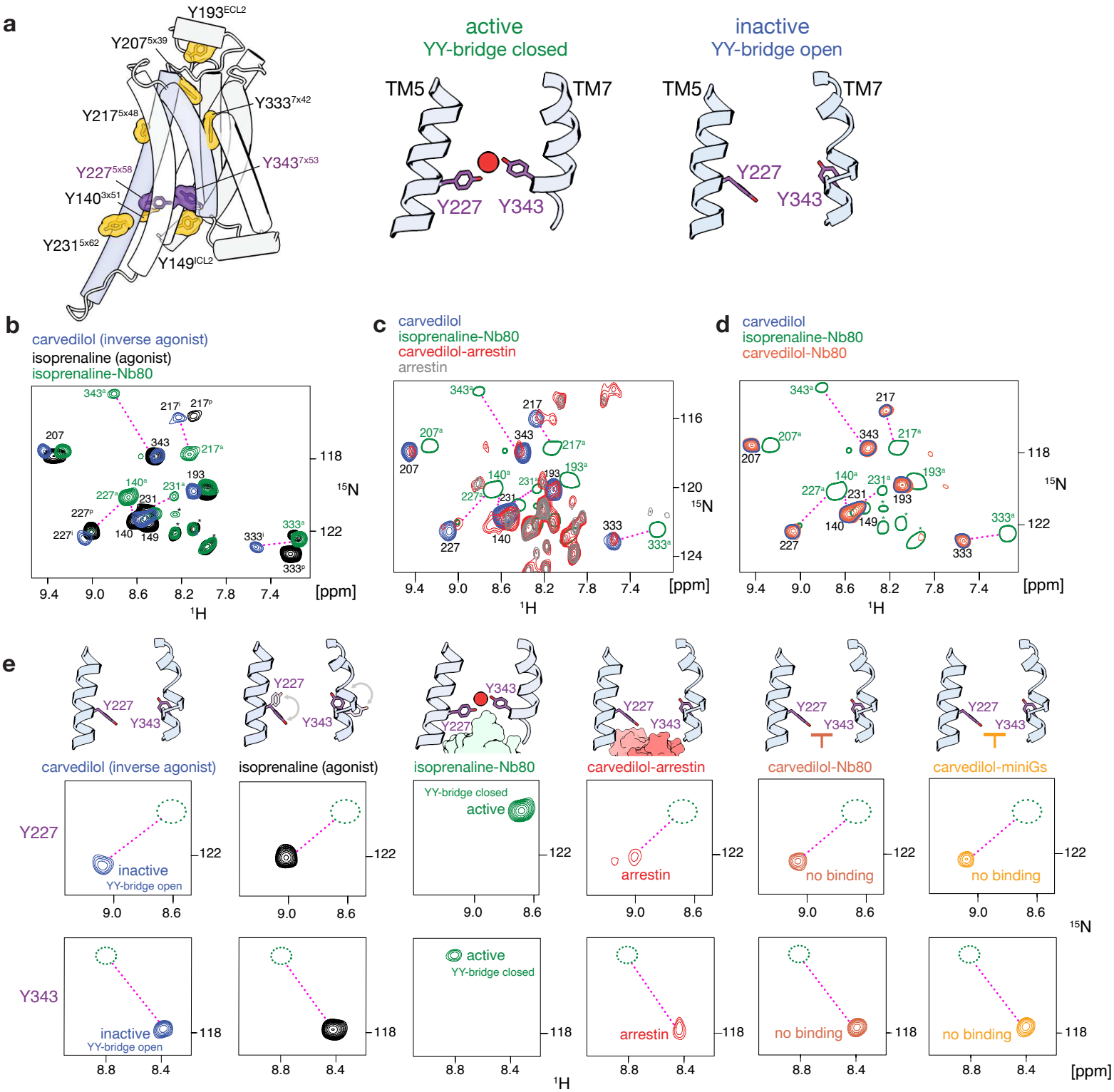
a
Y193ECL2
Y207 5x39
Y217 5x48
Y333 7x42
Y227 5x58
Y343 7x53
Y140 3x51
Y231 5x62
Y149ICL2
active
YY-bridge closed
TM5
TM7
Y227
Y343
inactive
YY-bridge open
TM5
TM7
Y227
Y343
b
carvedilol (inverse agonist)
isoprenaline (agonist)
isoprenaline-Nb80
c
carvedilol
isoprenaline-Nb80
carvedilol-arrestin
arrestin
d
carvedilol
isoprenaline-Nb80
carvedilol-Nb80
[ppm]
15N
1H
e
carvedilol (inverse agonist)
isoprenaline (agonist)
isoprenaline-Nb80
carvedilol-arrestin
carvedilol-Nb80
carvedilol-miniGs
Y227
Y343
inactive
YY-bridge open
YY-bridge closed
active
arrestin
no binding
[ppm]

Figure 3

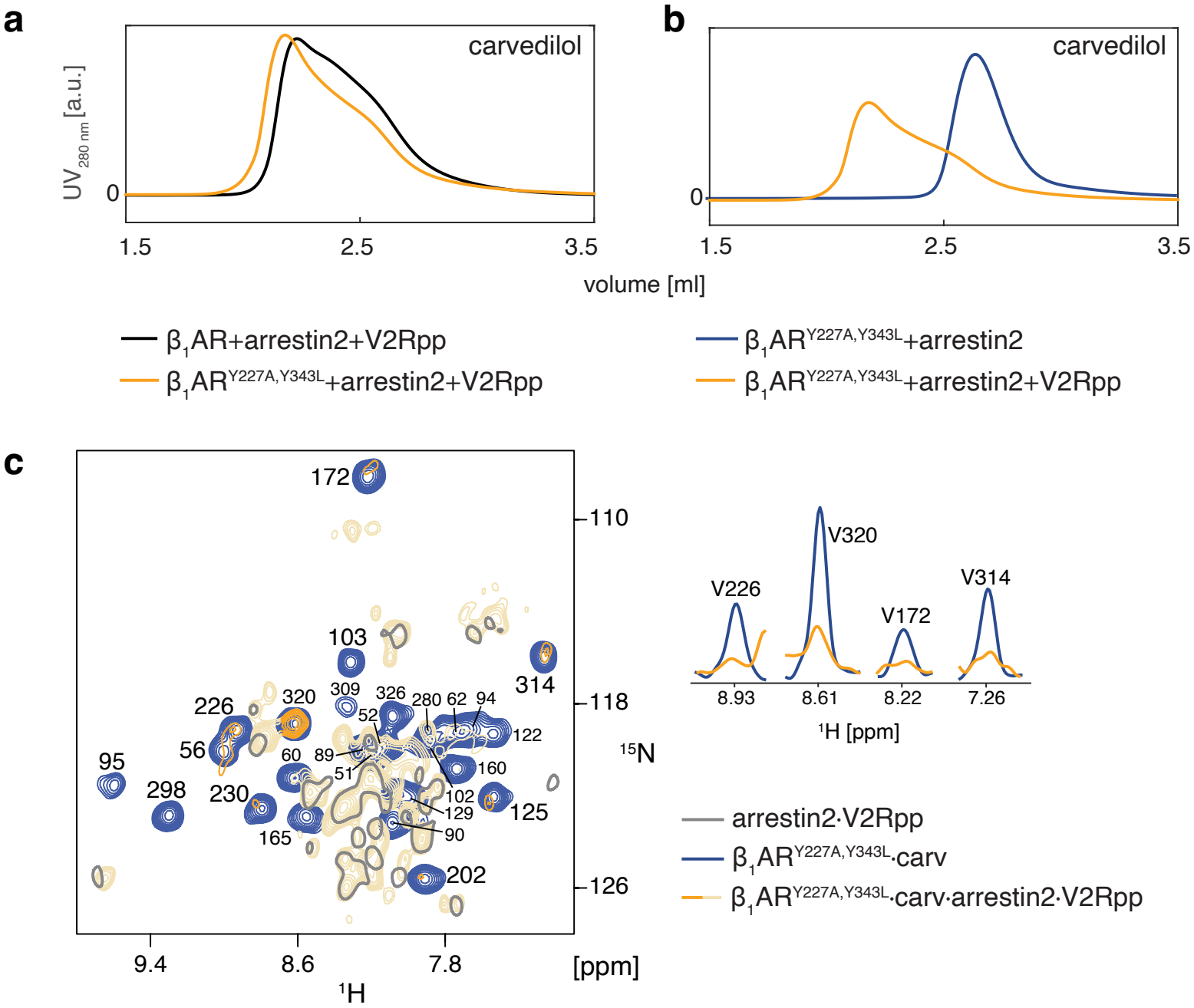
a
carvedilol
UV280 nm [a.u.]
0
1.5
2.5
3.5
volume [ml]
β1AR+arrestin2+V2Rpp
β1ARY227A,Y343L+arrestin2+V2Rpp
b
carvedilol
0
1.5
2.5
3.5
β1ARY227A,Y343L+arrestin2
β1ARY227A,Y343L+arrestin2+V2Rpp
c
172
110
103
314
118
226
320
309
326
280
62
94
52
122
56
60
89
51
160
95
298
230
102
129
125
165
90
202
126
15N
9.4
8.6
7.8
[ppm]
1H
V226
V320
V172
V314
8.93
8.61
8.22
7.26
1H [ppm]
arrestin2·V2Rpp
β1ARY227A,Y343L·carv
β1ARY227A,Y343L·carv·arrestin2·V2Rpp

Figure 4

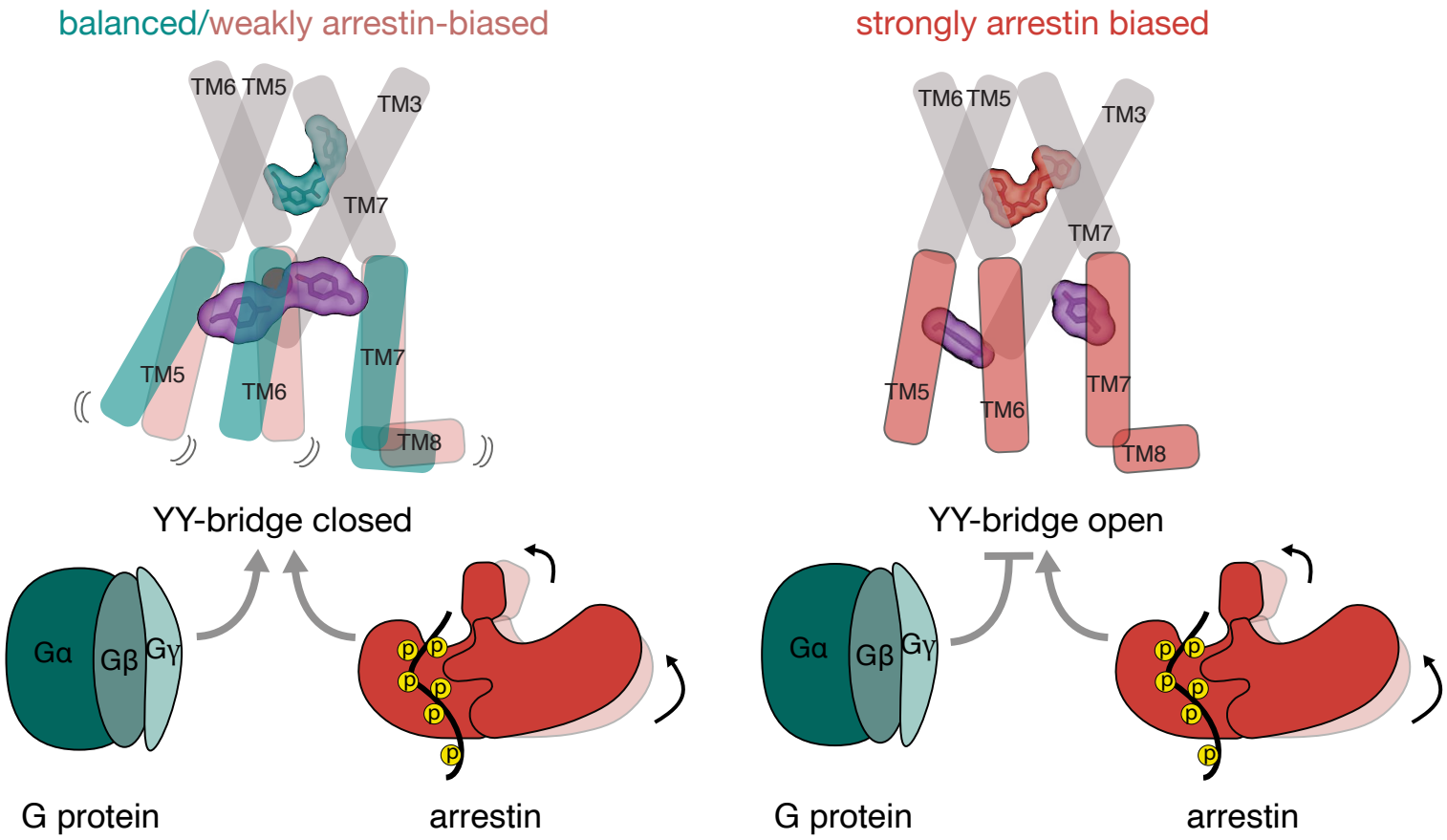
balanced/weakly arrestin-biased
TM6 TM5
TM3
TM7
TM5
TM6
TM7
TM8
YY-bridge closed
Gα
Gβ
Gγ
p
G protein
arrestin
strongly arrestin biased
TM6 TM5
TM3
TM7
TM5
TM6
TM7
TM8
YY-bridge open
Gα
Gβ
Gγ
p
G protein
arrestin

Figure 5